ATOMISTIC AND MESOSCOPIC MODELLING OF ELECTRIC CHARGE EVOLUTION IN POLYMERS

Marta M. D. Ramos[1] – A. M. Almeida[1] - J. P. M. Carneiro[1] – A. M. Stoneham[2]
[1]Departamento de Física, Universidade do Minho, Largo do Paço, 4700-320 Braga (P)
[2]Centre for Materials Research, Department of Physics and Astronomy, University College London, Gower Street, London WC1E 6BT (UK)

We address some of the issues relating to charge transport in polymer based devices. We examine the effects of variable chain length on both intramolecular and intermolecular bipolar charge transport in polydiacetylene (PDA) and poly(para-phenylenevinylene) (PPV), which should apply more widely to other polymer systems. Self-consistent quantum molecular dynamics calculations have been used to provide information on charge transport properties of individual polymer strands. Generalised Monte-Carlo calculations, with specific description of the ensemble of polymer strands, have been used to assess the effects of texture on the competition between charge transport, trapping and recombination across the polymer slab. Our results show an unanticipated but important effect from relatively long-lived yet transient trapping.

Introduction

Although continuum macroscopic models have been widely used to predict charge injection and transport in polymer based devices, the charge transport mechanism is still far from being well understood. This is due to the complexity of the charge transport process in the polymeric system where intramolecular, intermolecular, inter-domain and interfibrillar processes all contribute somewhat to the overall process.

Charges injected into individual molecular strands induce atomic and electronic relaxation processes. Information about the resulting states is obtained from atomic scale calculations, using self-consistent quantum molecular dynamics methods. The changes have been studied mainly for conjugated polymers [1-6], but similar charge-induced defects have been predicted for polymer wide-band-gap insulators, such as polystyrene [7]. These atomic scale calculations can determine the charge distribution associated with both the positive and the negative charge-induced defects in various polymer strands and their intramolecular mobility, when a bias voltage is applied. However, they cannot handle the complex charge transport phenomena, mentioned above, which occur at mesoscopic length and time scales.

Therefore, one needs to carry over the knowledge gained from atomic scale calculations into the mesoscopic regime. By suitable Monte-Carlo calculations, one can monitor collective charge transport through several realisations of polymer microstructures [8-11]. These mesoscopic simulations would provide information how the local morphology affects charge injection, transport, trapping and recombination in polymer based devices. Results of these calculations can be translated directly into information that is relevant to the engineering word (macroscopic length scale), e.g. controlled design of polymer microstructures for a range of applications.

We address here some of the issues relating to bipolar charge transport in polymers. At the molecular level, we shall exploit the self-consistent quantum molecular dynamics approach to describe the structures of charge-induced defects in polydiacetylene (PDA) and poly(para-phenylenevinylene) (PPV) and also study their intramolecular mobility. Since both charge injection from the appropriated electrode and charge tunnelling from one polymer strand to another is driven by the chemical potential difference, we shall examine the variation of chemical potential of PDA and PPV chains as a function of chain length. Other issues relevant to the charge transport efficiency are the effects due to variable charge injection sites in the polymer and the effects arising from the spatial molecular disorder which will be approached at the mesoscopic level. The present work examines the bipolar charge transport in inhomogeneous

polydiacetylene layers as a result of a nematic alignment of polymer strands with variable length. Our results concentrate on three factors: the effects of varying the proportion of short chains, the effects of varying the fraction of charge injection sites at polymer-electrode interface, and the effects of inert spherical inclusions.

Computational methods and models

For conducting polymer systems, where atomic positions and electronic structure are intimately coupled, methods combining molecular dynamics with self-consistent quantum mechanics techniques need to be used to study charge injection, transport and recombination at molecular level. The approach we adopt incorporates electronic structure effects into molecular dynamics through a semi-empirical application of the Hartree-Fock theory working at CNDO (Complete Neglect of Differential Overlap) level, which is the simplest semi-empirical method capable of dealing with relatively large systems in a self-consistent manner. Once the self-consistent inter-atomic forces are known, numerical integration of Newton's equation for all polymer atoms is performed to follow the atom trajectories in time.

In our mesoscopic model we describe the polymer layer as a stack of eight discrete molecular sub-monolayers sandwiched between the anode and the cathode. The minimum distance between two neighbouring sub-monolayers is 1nm. Each straight polymer strand is assumed to have six nearest neighbours (four in the same sub-monolayer and one in each of the two neighbouring sub-monolayers, respectively). Within each sub-monolayer, inter-chain distances ranging from 0.7 to 1.4 nm were used. The number of repeated units in each polymer strand not directly contacting an electrode varies with uniform probability from 2 to 20. All polymer strands bonded to the electrodes have 20 units. Our present work adopts molecular assemblies with an average degree of alignment perpendicular to both electrodes.

In order to model the transport of charge through the PDA chain network realisations, we have devised suitable rules for charge injection, transport and electron-hole recombination [9]. Firstly, we consider the injection of an equal number of electrons and holes at the same time. The injection of electrons (holes) occurs through polymer strands in contact with the negative (positive) electrode. We also assume that a certain fraction of polymer strands at each electrode are unfavourable to both electron and hole exchange. Secondly, we calculate the local electric field at each polymer strand (i.e. the superposition of the externally applied field of 2×10^8 V/m [12], the field of the other charges within the polymer network and the field due to electrode polarisation) which is responsible for the charge carrier drift. The charge injected at one of the chain ends moves instantaneously to the other end if it is favoured by the local electric field. We assume there is no electric field threshold for this intramolecular charge transport. In addition to intramolecular transport, charge carrier motion by an intermolecular hopping process can occur if the greatest hopping probability per time-step, calculated by the method given in reference [9], is more than 10^{-5}. Finally, recombination is considered to occur when two oppositely charge carriers meet on the same chain. Following Sixl [13], we have assumed radiative recombination at PDA chains with less than 9 repeated units.

Results and discussion

The ground state geometries of individual strands of PDA and PPV were found by examining straight molecules of $C_{4n+2}H_{2n+2}$ and $C_{8n}H_{6n+2}$, respectively, where n is the number of repeat units in each chain. Since the ground state carbon-carbon bond lengths of these polymers alternate along the chain, their dimerisation patterns can be defined by the absolute value of the difference between adjacent carbon-carbon bond lengths at each carbon atom. The ground state dimerisation patterns of PDA and PPV (***fig. 1***) are not as smooth as in trans-polyacetylene [2], because there are several inequivalent carbon-carbon bonds in these polymers. The dimerisation is slightly changed at the ends of both polymer chains.

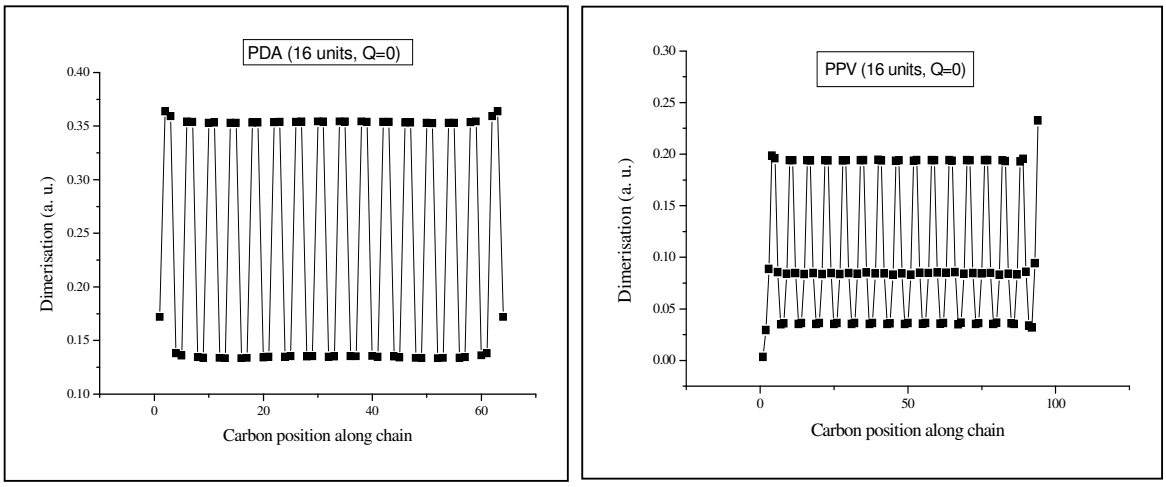

Fig. 1
Ground state dimerisation pattern of an isolated PDA (left-hand side) and PPV (right-hand side) chain with 16 repeat units. The line is a guide to the eye.

The injection of a single charge (electron or hole) to PDA and PPV chains leads to a charge-induced structural changes of the polymers backbone (***fig. 2***) which are accompanied by a local change in the electronic structure of the polymer. Both charge-induced defects are predicted to affect the chain length. This charge-induced distortion lengthens the multiple bonds and shortens the single bonds in the central region of both polymer chains. This structural defect position is energetically more favourable. The width of the distortion in dimerisation for charged PDA is rather greater than that of its equivalent in PPV. This is probably due to a reduced strength of the confinement in PDA. Besides, they have different amplitudes and shapes.

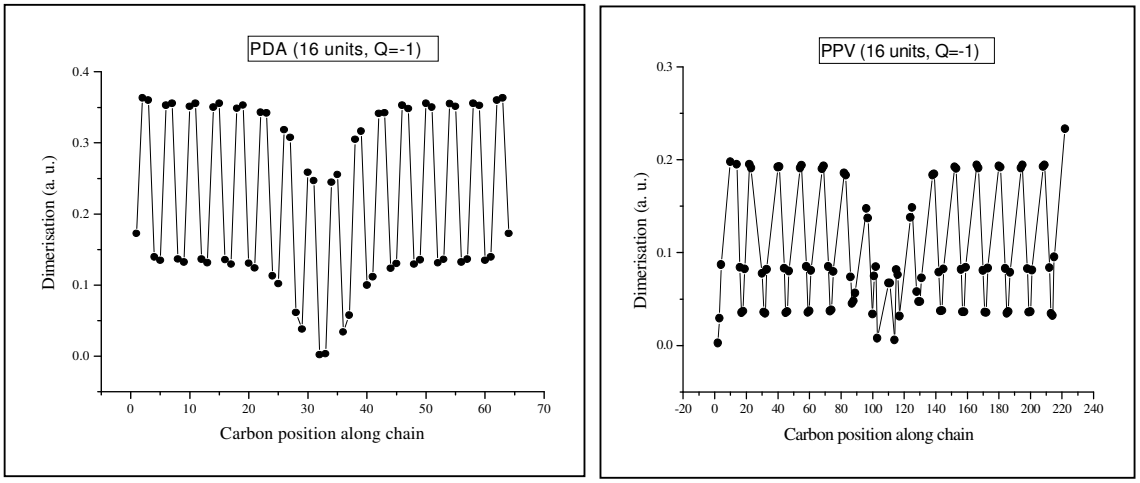

Fig. 2
Dimerisation pattern of a single negative charged PDA (left-hand side) and PPV (right-hand side) chain with 16 repeat units. The extent of the distortion is represented by the change in dimerisation patterns from their ground state values. The line is a guide to the eye.

For both positive and negative charged PDA and PPV chains, the injected charge is mainly stored on the carbon atoms. Our results also suggest a charge alternation on carbon atoms, whereas the charge stored on hydrogen atoms does not display this alternation (***fig. 3***). The charge alternation on carbon atoms predicted for PDA and PPV charged defects resembles those for polaron and soliton defects in trans-polyacetelyne [4]. The free-defect chains of PDA and PPV do not shown any charge alternation for hydrogen and carbon atoms.

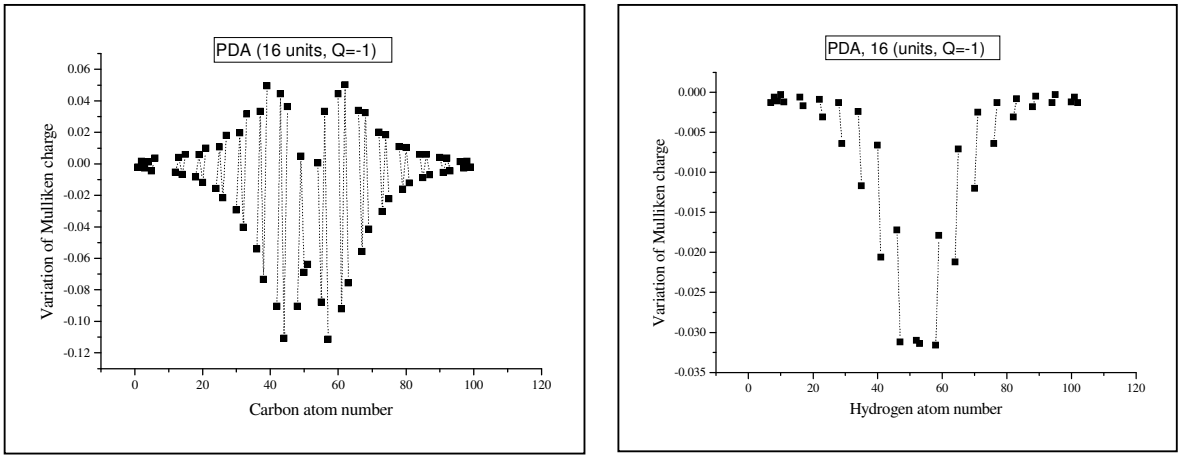

Fig. 3
Changes in Mulliken charges for carbon (left-hand side) and hydrogen (right-hand side) atoms of a single negative charged PDA chain with 16 repeat units. The line is a guide to the eye.

Before we deal with charge injection in the polymer network, we must consider the chemical potential of each polymer strand, since chemical potential differences drive electron transfer. Electrons tend to flow from a strand of high chemical potential to a strand of low chemical potential. The number of electrons that flow is to first order proportional to the chemical potential difference. The chemical potential is the negative of the electronegativity of Mulliken [14], which measures not only the difficulty of removing an electron from the strand but also the ease of gaining one. Thus, the molecular chemical potential, μ, can be determined from an arithmetic mean of the ionisation potential, I, and electron affinity, A, of a certain polymer chain:

$$\mu = -\frac{I + A}{2} \qquad (1)$$

For PDA the calculated chemical potential decreases with chain size to a nearly constant value for large chains (***fig. 4***). For PPV negligible change of molecular chemical potential is predicted. Using Koopmans' theorem [15], i.e., orbitals unchanged on ionisation, one finds approximately

$$\mu \approx \frac{E_{HOMO} + E_{LUMO}}{2} \qquad (2)$$

where E_{HOMO} and E_{LUMO} are the one-electron orbital energies of the highest occupied and lowest unoccupied orbitals, respectively. This equation can be considerably in error for short chains because the molecular charge change leads to a substantial change in the wave-functions. For PDA and PPV the two approaches agree for large chains (***fig. 4***). In fact, the chemical potential difference predicted by equations (1) and (2) is less than 0.3 eV.

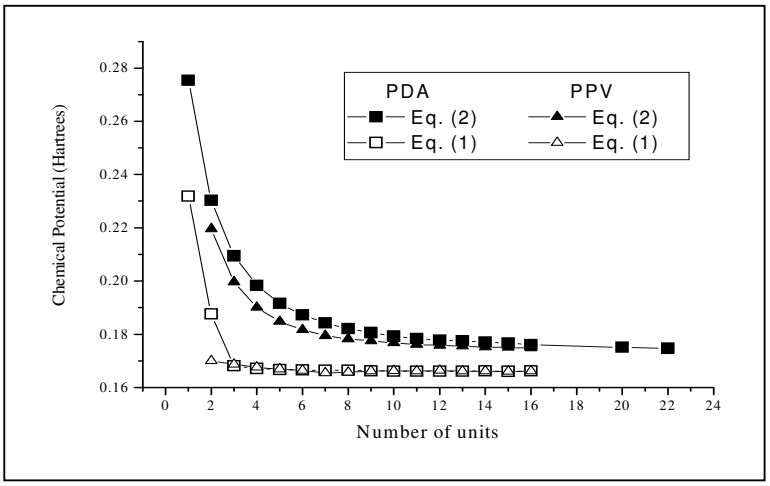

Fig. 4

Variations of the chemical potential of PDA (squares) and PPV (triangles) as a function of chain length. The open marks are obtained from equation (1) and the close marks are obtained from equation (2). The lines are a guide to the eye.

Even though the chemical potentials of PDA and PPV are rather similar for long chains, their electric field threshold for intramolecular charge transport at large chains is completely different. The threshold for charge mobility in PPV is just below $2x10^8$ V/m whereas PDA has a higher threshold. This has major implications for charge transport at mesoscopic level, which has not being considered in our mesoscopic model. However, the model can easily be modified to include such atomic scale effects.

Our molecular chemical potential results also suggest that, in some polymers, short strands may never play a part in the charge transport process, since the energetic barriers for charge injection at the electrode interface and intermolecular hopping processes may be relatively high. Besides, a large fraction of the injected charge on short chains returns to the electrode, as the image potential caused by the charge carriers themselves leads to a decrease in charge injection efficiency. The same effect has been reported for polymer contact electrification [16].

The injection efficiency can be varied in our mesoscopic model by adjusting the fraction of chargeable polymer strands. Our results (***fig. 5***) show a trapping increasing with reducing

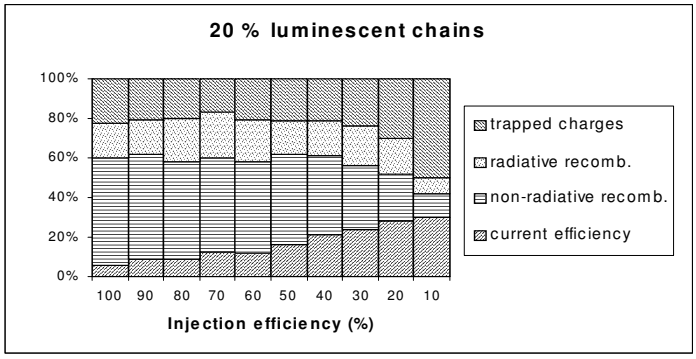

Fig. 5 *Proportions of injected charge which are trapped, recombine radiatively or non-radiatively or which cross the PDA network to carry a current, versus injection efficiency.*

injection efficiency. The total recombination and non-radiative recombination both anti-correlate

with trapping, whereas radiative recombination remains roughly constant for injection efficiencies greater than 20%. The competition between trapping and recombination leads to an increase in current efficiency (fraction of charge carriers reaching their target electrode) with reducing injection efficiency. This effect could not have been predicted before the computer simulations, and it suggests that filamentary conduction through the chain polymer network may be present. The effects of charge injection efficiency on current, recombination and trapping efficiencies are largely independent of the fraction of luminescent chains.

Chain networks with different densities were obtained in two ways, either changing the relative numbers of shorter (luminescent) chains and longer chains or by removing polymer strands and replacing them by spherical inclusions of inert material. For both types of network configuration, there is a general tendency for trapping to fall with increasing polymer density (***fig. 6***). The trapping efficiency within the chain polymer network is highest for the composite configuration. This result agrees with the expected behaviour: the transport of charge carriers within the network should be reduced by the existence of a smaller number of potential routes from electrode to electrode.

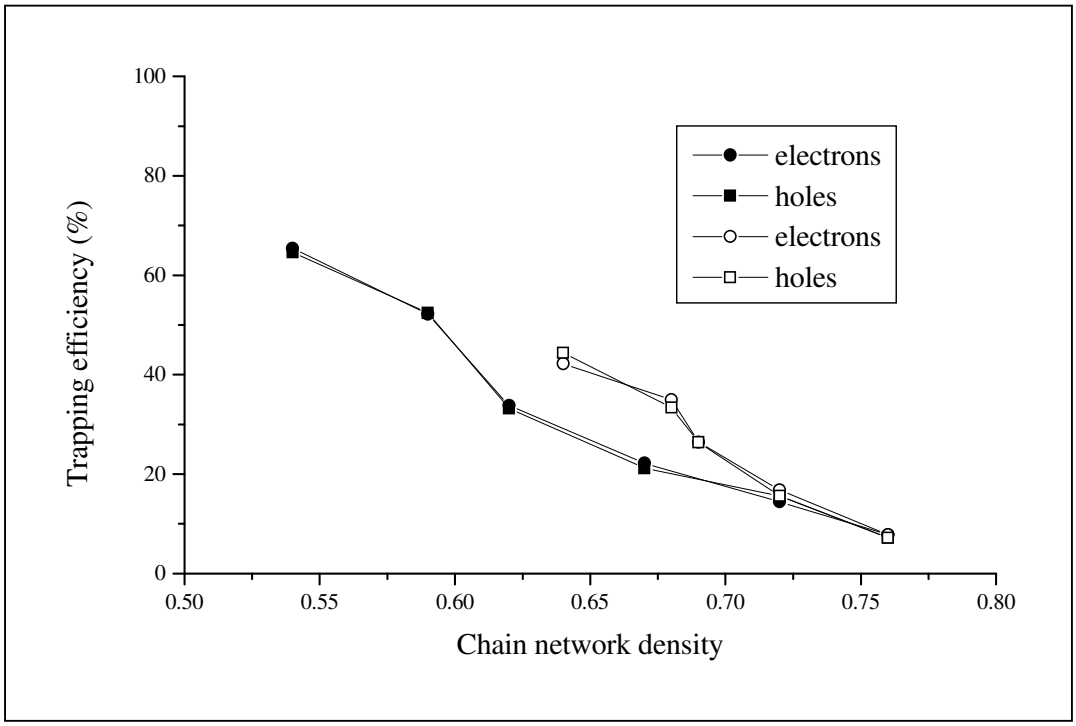

Fig. 6
Charge trapping efficiency as a function of PDA network density containing a variable fraction of: (a) luminescent strands (close marks); (b) spherical inert inclusions (open marks). The lines are a guide to the eye.

As chain network density decreases total recombination also decreases (***fig. 7***), since charge trapping becomes more important. Total recombination falls more rapidly with the number of inclusions than with the fraction of luminescent (short) chains. Since charge trapping and recombination have an opposite behaviour, current efficiency only increases slightly as chain network density increases (***fig. 8***) for both chain network configurations considered here. The effects on current efficiency due to the mesostructure are shown to be almost insignificant.

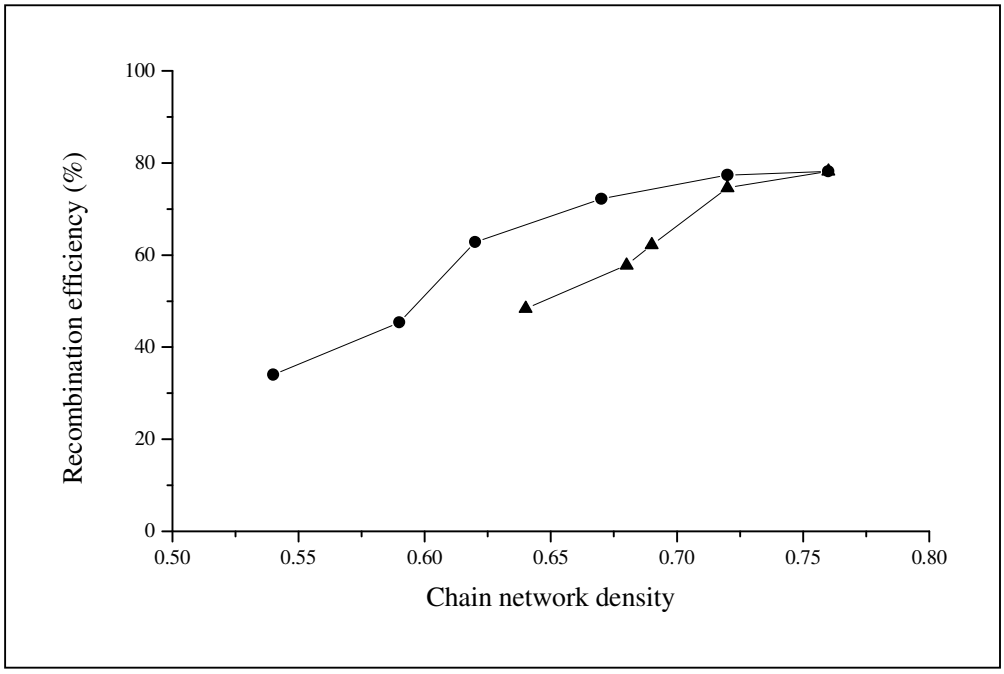

Fig. 6
Total recombination efficiency versus PDA network density for varying fractions of luminescent strands (circles) and spherical inert inclusions (triangles). The lines are a guide to the eye.

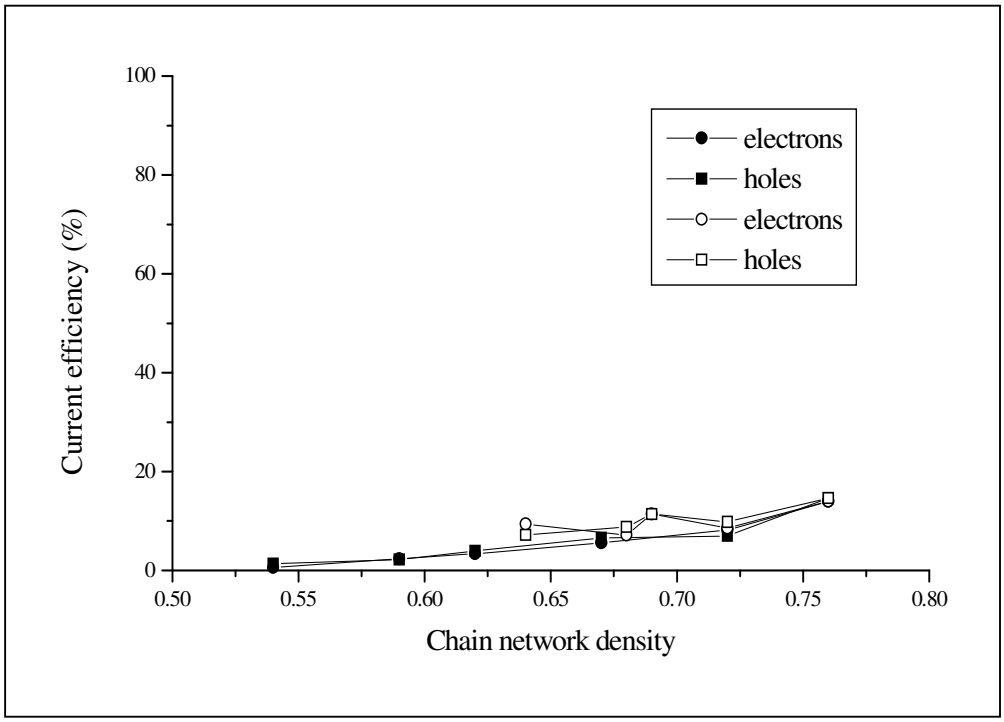

Fig. 7
Current efficiency versus PDA network density for varying fractions of luminescent strands (closed symbols) and spherical inert inclusions (open symbols). The lines are a guide to the eye.

Conclusions

Our approach to the atomistic and mesoscopic modelling of charge transport in conjugated polymers can also be applied to a large variety of polymer materials and different microscopic structures. We have used the models have been used to shed light on the relationship between the structure and transport properties of low band-gap polymers and to establish differences from conventional amorphous and crystalline semiconductors. Both approaches incorporate some standard components, such as quantum molecular dynamics and Monte-Carlo methods. Our mesoscopic approach can easily be modified to include input from computer experiments on polymer behaviour at atomic scale, as well as to allow multiple charge to be injected in a sequence of events. These generalisations would probably improve quantitative predictions of the transient trapping. Yet we believe the qualitative results to be reliable, and these show important features. One striking result is the increase of current efficiency at a small charge injection efficiency, despite the building-up transient space charge within the polymer layer.

REFERENCES

[1] D.S. Wallace, A.M. Stoneham, W. Hayes, A. Fisher, A. Testa - J. Phys.: Condens Matter, 3, 3905-3920, (1991).
[2] M.M.D. Ramos, A.M. Stoneham, A.P. Sutton - Synth. Met., 67, 137-140, (1994).
[3] M.M.D. Ramos, J.P.P. Almeida - Comput. Mater. Sci.,10,184-187, (1998).
[4] M.M.D. Ramos, J.P.P. Almeida - J. Mater. Process. Technol., 92-93, 147-150, (1999).
[5] A.M. Almeida, M.M.D. Ramos - Synth. Met.,122, 165-167, (2001).
[6] A.M. Almeida, M.M.D. Ramos - Vacuum,at press, (2001).
[7] C.B. Duke, T.J. Fabish – Phys. Rev. Lett., 37, 1075-1078, (1976).
[8] M.M.D. Ramos, A.M. Stoneham - Proc. 3rd Int. Conf. On Electric Charge in Solid Insulators, CSC'3, 59-65, (1998).
[9] M.M.D. Ramos, A.M. Stoneham - Comput. Mater. Sci.,17,260-264, (2000).
[10] M.M.D. Ramos, A.M. Stoneham - Synth. Met., 122, 149-151, (2001).
[11] A.M. Stoneham, M.M.D. Ramos - J. Phys.: Condens Matter, 13, 2411-2424, (2001).
[12] J. H. Burroughes, D. C. Bradley, A. R. Brown, R. N. Marks, K. Mackay, R. H. Friend, P. L. Burns and A. B. Holmes - Nature, 347, 539-541,(1990).
[13] H. Sixl - Polydiacetylene, pp. 240-245, Nijhoff, Amesterdam, (1984).
[14] R.S. Mulliken - J. Chem. Phys., 2, 782-793, (1934).
[15] T. Koopmans - Physica, 1, 104-113, (1934).
[16] W. J. Brennan, J. Lowell, G. W. Fellows, M. P. W. Wilson – J. Phys. D: Appl. Phys., 28, 2349-2355, (1995).